Research Article

Yuru Ge, Md. Ikram Ul Hoque*, and Qunting Qu

1D Hematite-[α-Fe_2O_3]-nanorods prepared by green fabrication for supercapacitor electrodes

https://doi.org/10.1515/eetech-2019-0001
Received Apr 10, 2019; accepted May 13, 2019

Abstract: 1D α-hematite nanorods synthesized by a simple, scalable and novel green chemistry method exhibit fast kinetics of the interfacial Faradaic redox reaction yielding a specific capacitance of 140 $F{\cdot}g^{-1}$ when used as a battery-type electrode in a supercapacitor. Ample supply and environmental compatibility of the raw material suggest the use of this material. Insufficient stability suggest further investigations.

Keywords: α-hematite, nanorods, 1D material, supercapacitor

1 Introduction

Green chemistry routes to one-dimensional (1D) iron oxide-based nanomaterials are attractive because of their low environmental impact and the superior physicochemical properties of the products compared to two-dimensional (2D) and three-dimensional (3D) iron oxide nanoparticles. 1D iron oxides are categorized into nanorods, nanotubes, nanoneedles, nanofibers and nanowires. Nanostructuring of active masses as electrode materials of batteries and supercapacitors has been suggested frequently because of beneficial effects of nanostructuring on material performance [1–4]. Because of the large resources and in particular its environmental compatibility iron and its compounds are attractive materials for electrodes in devices for electrochemical energy conversion [5–9]. The polymorphs of iron oxides are hematite (α-Fe_2O_3), beta hematite (β-Fe_2O_3), epsilon hematite (ϵ-Fe_2O_3) maghemite (γ-Fe_2O_3), and magnetite (Fe_3O_4).

Because of its ample supply and environmental compatibility iron and its oxide have been considered very early as active masses for batteries

The number of reports on iron-containing (mostly iron oxides and hydroxides) supercapacitor electrode materials is substantial (until 03/2019 about 900), but only few studies of hematite (α-Fe_2O_3) mostly employing this material in the negative electrode as implied in the overview provided by Qu *et al.* [10] have been published. Sarma *et al.* [11] prepared iron oxide nanotubes (a mixture of hematite and Fe_3O_4) with fairly moderate performance data. Nanotube hematite arrays prepared by Xie *et al.* [12] showed 138 $F{\cdot}g^{-1}$ with 89% of the initial capacitance left after 500 cycles. Mixed porous iron oxide films containing nanorods and nanosheets with a specific capacitance < 100 $F{\cdot}g^{-1}$ have been described by Wu and Lee [13]. Shivakumara *et al.* [14] have reported on porous flowerlike hematite nanostructures providing a specific capacitance of 127 Fg^{-1} with a capacitance retention of about 80% after 1000 cycles.

Iron oxide nanoparticles composed of α-FeOOH/Fe_2O_3 synthesized in a one-step process by Barik *et al.* [15] showed 160 $F{\cdot}g^{-1}$ with the former and 200 $F{\cdot}g^{-1}$ for the latter material. Using a sol-gel process, Shivakumar *et al.* [16] prepared porous hematite providing a capacitance of 193 $F{\cdot}g^{-1}$ with 92% capacitance retention after 1000 cycles. Various hematite morphologies were obtained by a solution-based precipitation process starting with iron oxalate [17]. In this case, a maximum specific capacitance of 116.25 $F{\cdot}g^{-1}$ and moderate cycling stability were found. Reports on the use of various morphologies of iron oxides have been provided [18–24], reviews on iron oxide and iron hydroxide-based materials for supercapacitor electrodes are available [25, 26].

Carbon-coated hematite nanoparticles prepared in a one-step self-assembly process by Yan *et al.* [27] provided a specific capacitance of 406.9 $F{\cdot}g^{-1}$ with 90.7% retention after 2000 cycles. Gannavarapu and Dandamudi [28] obtained a nano iron oxide supported on activated carbon composite showing a capacitance of 898 $F{\cdot}g^{-1}$ with 95% capacitance retention after 10000 cycles. Yan *et al.* have

***Corresponding Author: Md. Ikram Ul Hoque:** Discipline of Chemistry, University of Newcastle, University Drive, Callaghan, NSW 2308, Australia; Department of Chemistry, Dhaka University of Engineering & Technology, Gazipur, Gazipur-1700, Bangladesh; Email: md.ikramul.hoque@uon.edu.au; ikram_chem_ju@yahoo.com
Yuru Ge: Technische Universität Chemnitz, Institut für Chemie, AG Elektrochemie, D-09107 Chemnitz, Germany
Qunting Qu: College of Physics, Optoelectronics and Energy, Soochow University, Suzhou, Jiangsu 215006, P. R. China

prepared a carbon-coated cocoon-like hematite composite with a specific capacitance of 601 at 1 $A \cdot g^{-1}$ [29]. Graphene sheets decorated with hematite quantum dots showing a specific capacitance of 347 $F \cdot g^{-1}$ have been reported [30]. Magnetite nanoparticles used as active material in a supercapacitor electrode with specific capacitances ranging from 30 to 510 $F \cdot g^{-1}$ depending on the dispersion of the nanoparticles in the conductive matrix of carbon black have been observed by Wu *et al.* [31].

Peng *et al.* [32] prepared a composite of hematite nanocrystals and carbon cloth without need for a binder and a capacitance retention of 88.6% after 5000 cycles. An initial areal capacitance of 1.66 $F \cdot cm^{-2}$ was observed. Xie *et al.* deposited α-Fe_2O_3 on graphene oxide paper [33]. The material provided an areal capacitance of 3.08 $F \cdot cm^{-2}$; about 100% capacitance retention were noted after 5000 cycles. Lee *et al.* [34] prepared crumpled graphite loaded with various iron oxides (hematite and magnetite) with the magnetite-loaded material showing higher capacitance values. Bhattacharya *et al.* [35] have extracted hematite from industrial red mud, the obtained material provided $\approx$ 317 $F \cdot g^{-1}$ with $\approx$ 97% capacitance retention after 5000 cycles.

Expecting potential advantages of a 1D-structured hematite, we have examined 1D-nanorods of hematite for the first time in the study reported here. A report on the green synthesis and extensive characterization of the material examined here has been provided elsewhere [36].

2 Experimental

2.1 Chemicals and reagents

All chemicals used in this research were of analytical grade. Potassium hydroxide (Grüssing) were purchased from Merck, Darmstadt, Germany. Electrolyte solutions were prepared with ultrapure 18 MΩ water (Seralpur Pro 90 C). Acetylene black and poly(tetrafluoroethylene) (PTFE, 60 wt% dispersion in H_2O) were purchased from Shanghai Haohua Chemical and Industrial Co., Ltd and Sigma-Aldrich, respectively. Hematite nanorods were prepared elsewhere with all details including experimental ones reported [36].

2.2 Electrochemical tests

The working electrode was prepared as follows. A mushy mixture composed of hematite nanorods, acetylene black, and PTFE with a weight ratio of 7:2:1 dispersed in ethanol was prepared and pressed into a thin film. This was finally punched into small disks with a diameter of 10 mm. The disks were pressed onto a stainless steel grid (Stainless steel ss 1.4401 mesh 181 with 0.09 mm width and 0.05 mm thickness, supplied by F. Carl Schröter, Hamburg, Germany) at a pressure of 12 MPa and dried at 70°C. The loading with active hematite on each electrode was about 9 $mg \cdot cm^{-2}$. An aqueous electrolyte solution of 1 $mol \cdot dm^{-1}$ of KOH was used. Electrochemical testing was performed using a three-electrode cell containing a hematite working electrode, platinum sheet counter electrode, and saturated calomel reference electrode (SCE) with a potentiostat IVIUMSTAT Electrochemical Interface. Cyclic voltammetry (CV) data were collected between −0.3 and −1.2 V vs. SCE at various scan rates. Galvanostatic charge/discharge tests were performed at a current density of 1 $A \cdot g^{-1}$ within a potential window of −0.3 to −1.1 V vs. SCE.

3 Results and discussion

3.1 Material characterization

Rice starch acting as soft template in the fabrication process of the α-hematite nanorods was added at different percentages 0, 5, 10, 15 and 20% in solution. Corresponding SEM images are displayed in Figure 1A-E. They clearly show that starch played a crucial role in the growth of the nanorods. In the absence of starch, the initially formed $Fe(OH)_3$ gel yielded neither nanorods nor nanoparticles but lumps of iron (III) oxide moieties instead (Figure 1A). Already with 5% starch solution rod formation was observed (Figure 1B-E). To identfiy any effect of the starch content in solution on size, shape and surface morphology of the nanorods, the percentage of starch solution was increased. The size of the nanorods at 250 nm and 50 nm in length and diamete stayed approximately the same at all concentrations (Figure 1B-E). Surface appearance of the nanorods slightly changed from rough to smooth with the percentage of starch solution up to 15%, no further change was found at 20%. 15% starch cncentration was selected for the synthesis of the hematite nanorods for further study. The EDX data (Figure 1F) showed that only iron, oxygen and carbon were present in the hematite nanorods and their percentages of atoms were found to be 11.92, 59.17 and 28.91, respectively. The carbon may be left from the starch that was used as a soft template for the nanorod growth.

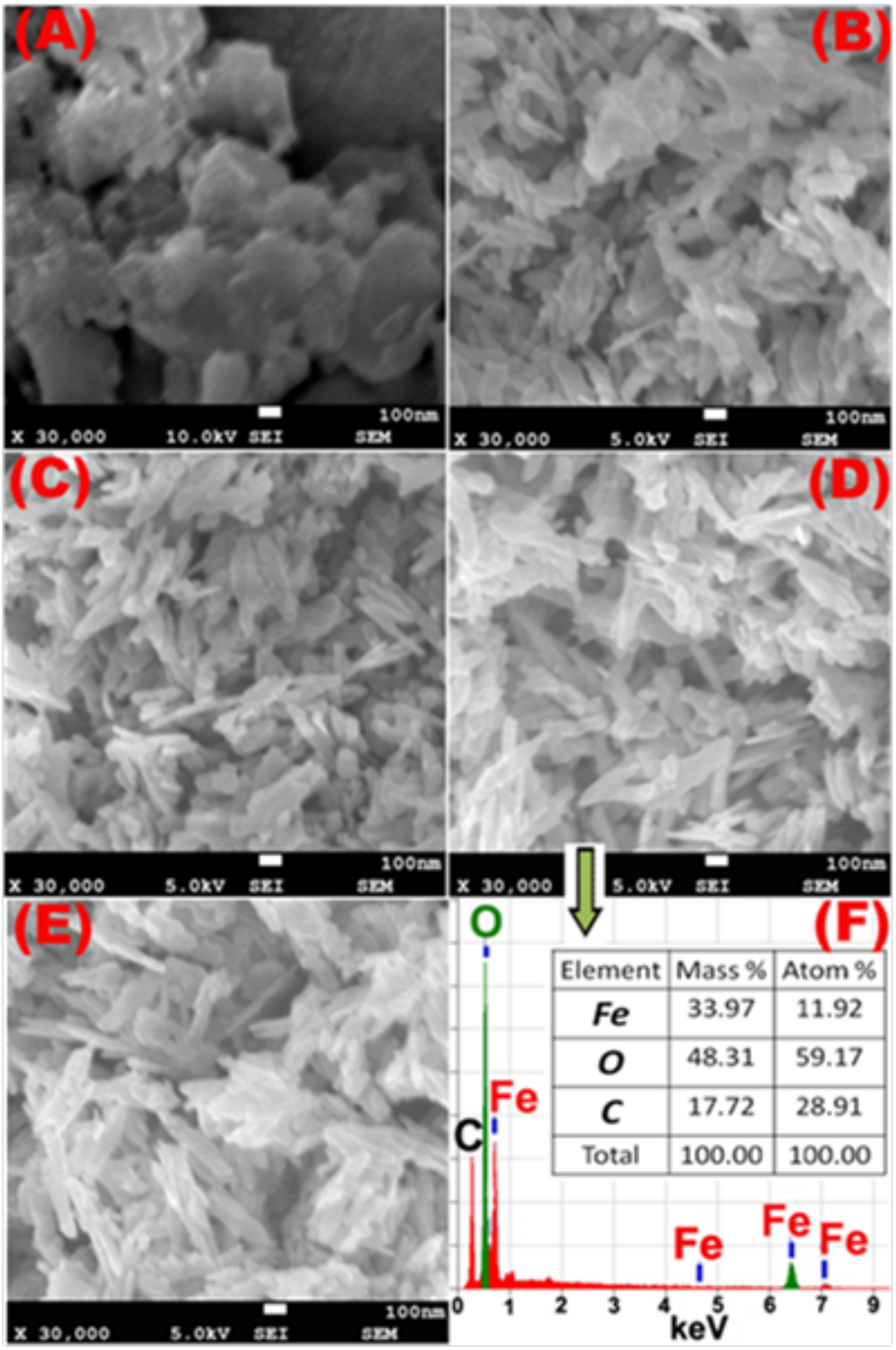

Figure 1: SEM images (A-E) of hematite nanorods obtained using different percentages of starch for the fabrication of, (A) 0%, (B) 5%, (C) 10%, (D) 15%, (E) 20% and (F) EDX spectrum of hematite nanorod fabricated using 15% starch (for details see [36]).

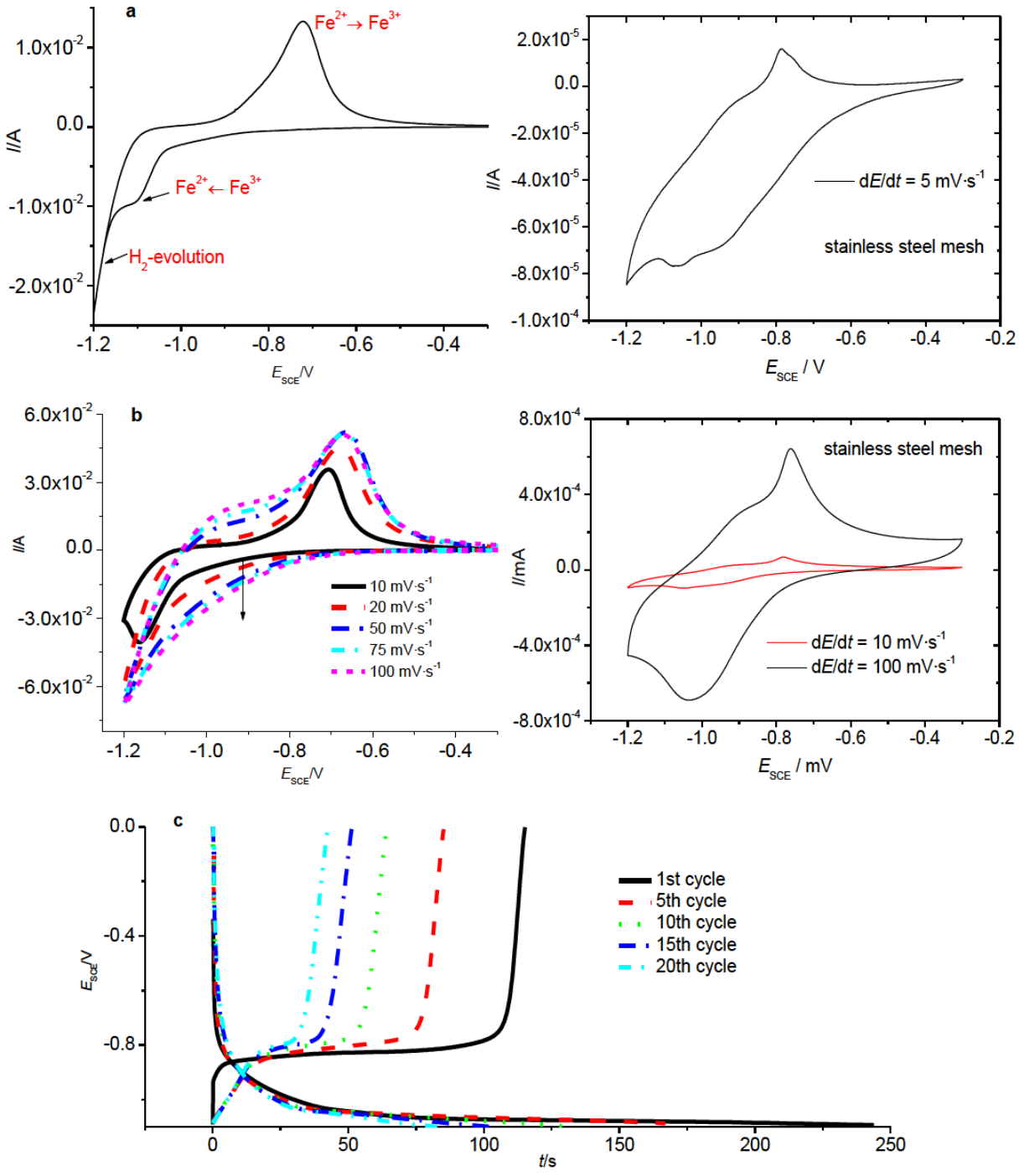

Figure 2: CVs of the hematite electrode (a) at a scan rate of 5 mV·s^{-1} and (b) at various scan rates ranging from 10 to 100 mV·s^{-1}. (c) The charge/discharge curves of a hematite electrode at different cycle numbers at a current density of 1 A·g^{-1}.

3.2 Electrochemical results

The CV of the hematite electrode at dE/dt = 5 mV·s^{-1} is shown in Figure 1a, one couple of redox peaks is clearly observed. The reduction peak at −1.1V is due to the electrochemical reduction of Fe^{3+} to Fe^{2+}, while the oxidation peak is caused by the oxidation of Fe^{2+} into Fe^{3+}. The appearance of such distinct redox peaks signals the battery electrode-like nature of hematite. For comparison the CV of the stainless steel mesh used as support is displayed in Figure 1a. It shows a redox couply typical of the iron dminating the chemical composition f the steel al-

loy. The current caused by this couple is orders of magnitude smaller and can safely be neglected in further discussion. Electrode potential and shape of the Fe^{2+}/Fe^{3+} redox peaks caused by the hematite resemble closely those of previously reported Fe_2O_3 nanoparticles [37] and graphite foam-carbon nanotube@Fe_2O_3 composites [38]. In addition, the CV of the hematite sample studied here is very similar to that of previously prepared FeOOH, which is transformed into Fe_3O_4 after electrochemical cycling in the anodic potential range $0 < E_{SCE} < -1.3$ V [10].

As the scan rate increases from 10 to 100 $mV \cdot s^{-1}$, the CVs shown in Figure 1b are obtained. The anodic peaks of hematite can be observed clearly even at the fast scan rate of 100 $mV \cdot s^{-1}$, indicating quite fast kinetics of the superficial redox reactions. The potential difference between the anodic and cathodic peaks in the CVs slightly increases owing to the increased polarization of the electrode reactions at faster scan rates. The galvanostatic charge/discharge curves at $j = 1\ A \cdot g^{-1}$ in different cycles are shown in Figure 1c. The obvious plateaus at around −0.8 V vs. SCE correspond well to the anodic peaks in the CV curves. Such electrode potential plateaus are also observed for other supercapacitive electrode materials such as Fe_3O_4 [10], Ni(OH) [39], and Co_3O_4 [40]; they suggest designation of the material examined here as "battery-electrode like". Although an ideal supercapacitive electrode material [41] should exhibit linear charge/discharge curves as observed with EDLC-supercapacitors, materials exhibiting obvious redox peaks or potential plateaus are also called supercapacitive materials because of their ultrafast superficial charge/discharge ability [?]. The specific gravimetric capacitance of the electrode can be calculated according to the formula reported elsewhere [10, 42]. The specific capacitance of hematite at the 1st, 5th, 10th, and 20th cycle is 140, 103, 76, and 49 $F \cdot g^{-1}$, respectively, manifesting a quite fast capacitance fading of hematite. Moreover, the overall capacitance is lower than that of carbon-coated cocoon-like-Fe_2O_3 nanocomposite (601 $F \cdot g^{-1}$ at 1 $A \cdot g^{-1}$) [29] Fe_2O_3 nanoparticles (716 $F \cdot g^{-1}$ at 1 $A \cdot g^{-1}$) [37], and Fe_2O_3 quantum dot/graphene-sheets (347 $F \cdot g^{-1}$ at a scan rate of 10 $mV \cdot s^{-1}$) [30]. The lower capacitance and fast capacity decay of hematite nanorods studied here may result from their low electronic conductance as well as the poor structural stability. Accordingly incorporation of other carbon materials into the synthesis of hematite and/or coating of the nanorods with carbon or an intrinsically conducting polymer (see [43, 44]), which is expected to enhance electronic conductance and structural stability possibly improving performance and longtime behavior, is under study now.

4 Conclusions

1D hematite nanorods were prepared by a green method and examined as active negative electrode mass for an aqueous supercapacitor. They provided a specific capacitance of 140 $F \cdot g^{-1}$ at $j = 1\ A \cdot g^{-1}$ showing insufficient cycling stability.

References

[1] Dubal D.P., Holze R., Synthesis, properties, and performance of nanostructured meal oxides for supercapacitors, Pure Appl. Chem., 2014, 86, 611-632.

[2] Zhang X., Cheng X., Zhang Q., Nanostructured energy materials for electrochemical energy conversion and storage: a review, J. Energy Chem., 2016, 25, 967-984.

[3] Jiang J., Zhang Y., Nie P., Xu G., Shi M., Wang J., Wu Y., Fu R., Dou H., Zhang X., Progress of nanostructured electrode materials for supercapacitors, Adv. Sust. Systems, 2018, 2, 1700110

[4] Zhang Q., Uchaker E., Candelaria S.L., Cao G., Nanomaterials for energy conversion and storage, Chem. Soc. Rev., 2013, 42, 3127-3171.

[5] Shukla A.K., Ravikumar M.K., Balasubramanian T.S., Nickel/iron batteries, J. Power Sources, 1994, 51, 29-36.

[6] Weinrich H., Come J., Tempel H., Kungl H., Eichel R.-A., Balke N., Understanding the nanoscale redox-behavior of iron-anodes for rechargeable iron-air batteries, Nano Energy 2017, 41, 706-716.

[7] Rajan A.S., Ravikumar M.K., Priolkar K.R., Sampath S., Shukla A.K., Carbonyl-iron electrodes for rechargeable-iron batteries, Electrochem. Energy Technol., 2014, 1, 2-9.

[8] Reddy T., Linden D., Linden's Handbook of Batteries, New York: McGraw-hill, 4, 2011

[9] Li J., Daniel C., Wood III D.L., Cathode Manufacturing for Lithium-Ion Batteries, Handbook of Battery Materials. 2011, 24, 939-60.

[10] Qu Q., Yang S., Feng X., 2d sandwich-like sheets of iron oxide grown on graphene as high energy anode material for supercapacitors, Adv. Mater., 2011, 23, 5574-5580.

[11] Sarma B., Jurovitzki A.L., Ray R.S., Smith Y.R., Mohanty S.K., Misra M., Electrochemical capacitance of iron oxide nanotube (Fe-NT): effect of annealing atmospheres, Nanotechnol., 2015, 26, 265401

[12] Xie K., Li J., Lai Y., Lu W., Zhang Z., Liu Y., Zhou L., Huang H., Highly ordered iron oxide nanotube arrays as electrodes for electrochemical energy storage, Electrochem. Commun., 2011, 13, 657-660.

[13] Wu M.S., Lee R.H., Electrochemical growth of iron Oxide thin films with nanorods and nanosheets for capacitors, J. Electrochem. Soc., 2009, 156, A737-A743.

[14] Shivakumara S., Penki T.R., Munichandraiah N., Synthesis and Characterization of Porous Flowerlike α-Fe2O3 Nanostructures for Supercapacitor Application, ECS Electrochem. Lett., 2013, 2, A60-A62.

[15] Barik R., Jena B.K., Dash A., Mohapatra M., In situ synthesis of flowery-shaped α-FeOOH/Fe2O3 nanoparticles and their phase dependent supercapacitive behaviour, RSC Adv., 2014, 4, 18827-18834.

[16] Shivakumara S., Penki T.R., Munichandraiah N., Preparation and electrochemical performance of porous hematite (α-Fe2O3) nanostructures as supercapacitor electrode material, J. Solid State Electrochem., 2014, 18, 1057-1066.
[17] Wang D., Wang Q., Wang T., Controlled synthesis of mesoporous hematite nanostructures and their application as electrochemical capacitor electrodes, Nanotechnol., 2011, 22, 135604
[18] Sun H., Chen B., Jiao X., Jiang Z., Qin Z., Chen D., Solvothermal synthesis of tunable electroactive magnetite nanorods by controlling the side reaction, J. Phys. Chem. C, 2012, 116, 5476-5481.
[19] Chen J., Huang K.L., Liu S.Q., Hydrothermal preparation of octadecahedron Fe3O4 thin film for use in an electrochemical supercapacitor, Electrochim. Acta, 2009, 55, 1-5.
[20] Wang S.Y., Ho K.C., Kuo S.L., Wu N.L., Investigation on capacitance mechanisms of Fe3O4 electrochemical capacitors, J. Electrochem. Soc., 2006, 153, A75-A80.
[21] Pang S.C., Khoh W.H., Chin S.F., Nanoparticulate magnetite thin films as electrode materials for the fabrication of electrochemical capacitors, J. Mater. Sci., 2010, 45, 5598-5604.
[22] Nagarajan N., Zhitomirsky I., Cathodic electrosynthesis of iron oxide films for electrochemical supercapacitors, J. Appl. Electrochem., 2006, 36, 1399-1405.
[23] Wang S.Y., Wu N.L., Operating characteristics of aqueous magnetite electrochemical capacitors, J. Appl. Electrochem., 2003, 33, 345-348.
[24] Wu M.S., Lee R.H., Jow J.J., Yang W.D., Hsieh C.Y., Weng B.J., Nanostructured iron oxide films prepared by electrochemical method for electrochemical capacitors, Electrochem. Solid-State Lett., 2009, 12, A1-A4.
[25] Xia Q., Xu M., Xia H., Xie J., Nanostructured Iron Oxide/Hydroxide-Based Electrode Materials for Supercapacitors, ChemNanoMat, 2016, 2, 588-600.
[26] Nithya V.D., Arul N.S., Review on α-Fe2O3 based negative electrode for high performance supercapacitors, J. Power Sources, 2016, 327, 297-318.
[27] Yan Y., Tang H., Wu F., Wang R., Pan M., One-step self-assembly synthesis α-Fe2O3 with carbon-coated nanoparticles for stabilized and enhanced supercapacitors electrode, Energies, 2017, 10, 1296
[28] Gannavarapu K.P., Dandamudi R.B., Shape engineered three dimensional α-Fe2O3-activated carbon nano composite as enhanced electrochemical supercapacitor electrode material, Int. J. Energ. Res., 2018, 42, 4687-4696.
[29] Y. Yan, H. Tang, F. Wu, R. Wang, M. Pan, One-step self-assembly synthesis α-Fe2O3 with carbon-coated nanoparticles for stabilized and enhanced supercapacitors electrode, Energies, 2017, 10, 1296.
[30] Xia H., Hong C., Li B., Zhao B., Lin Z., Zheng M., Savilov S.V., Aldoshin S.M., Facile Synthesis of Hematite Quantum-Dot/Functionalized Graphene-Sheet Composites as Advanced Anode Materials for Asymmetric Supercapacitors, Adv. Funct. Mater., 2015, 25, 627-635.
[31] Wu N.L., Wang S.Y., Han C.Y., Wu D.S., Shiue L.R., Electrochemical capacitor of magnetite in aqueous electrolytes, J. Power Sources, 2003, 113, 173-178.
[32] Peng S., Yu L., Lan B., Sun M., Cheng G., Liao S., Cao H., Deng Y., Low-cost superior solid-state symmetric supercapacitors based on hematite nanocrystals, Nanotechnol., 2016, 27, 505404
[33] Xie S., Zhang M., Liu P., Wang S., Liu S., Feng H., Zheng H., Cheng F., Advanced negative electrode of Fe2O3/graphene oxide paper for high energy supercapacitors, Mater. Res. Bull., 2017, 96, 413-418.
[34] Lee C., Jo E.H., Kim S.K., Choi J.-H., Chang H., Jang H.D., Electrochemical performance of crumpled graphene loaded with magnetite and hematite nanoparticles for supercapacitors, Carbon, 2017, 115, 331-337.
[35] Bhattacharya G., Fishlock S.J., Roy J.S., Pritam A., Banerjee D., Deshmukh S., McLaughlin J.A., Roy S.S., Effective Utilization of Waste Red Mud for High Performance Supercapacitor Electrodes, Global Challenges, 2018, 2018, 1800066
[36] Hoque M.I.U., Yamauchi Y., Naidu R., Holze R., Saidur R., Qu Q., Rahman M.M., Torad N.L., Hossain Md.S.A., Kim S., M., Kim J., Ahmad S.H.A., Rehman A. U., Firoz S.H., Luba U., Chowdhury S., Chowdhury A.-N., A Facile Synthesis of Hematite Nanorods from Rice Starch and Their Application to Pb (II) Ions Removal, Chemistry Select, 2019, 4, 3730-3736.
[37] Owusu K.A., Qu L., Li J., Wang Z., Zhao K., Yang C., Hercule K.M., Lin C., Shi C., Wei Q., Zhou L., Mai L., Low-crystalline iron oxide hydroxide nanoparticle anode for high-performance supercapacitors, Nat. Commun., 2017, 8, 14264
[38] Guan C., Liu J., Wang Y., Mao L., Fan Z., Shen Z., Zhang H., Wang J., Iron oxide-decorated carbon for supercapacitor anodes with ultrahigh energy density and outstanding cycling stability, ACS Nano, 2015, 9, 5198-5207.
[39] Ede S.R., Anantharaj S., Kumaran K.T., Mishra S., Kundu S., One step synthesis of Ni/Ni (OH)2 nano sheets (NSs) and their application in asymmetric supercapacitors, RSC Adv., 2017, 7, 5898-5911.
[40] Wang X., Li M., Chang Z., Yang Y., Wu Y., Liu X., Co3O4@ MWCNT nanocable as cathode with superior electrochemical performance for supercapacitors, ACS Appl. Mater. Interfaces, 2015, 7, 2280-2285.
[41] Holze R., From current peaks to waves and capacitive currents - on the origins of capacitor-like electrode behavior, J. Solid State Electrochem., 2017, 21, 2601-2607.
[42] Qu Q.T., Zhang P., Wang B., Chen Y.H., Tian S., Wu Y.P., Holze R., Electrochemical performance of MnO2 nanorods in neutral aqueous electrolytes as a cathode for asymmetric supercapacitors, J. Phys. Chem. C, 2009, 113, 14020-14027.
[43] Holze R., 9 - Metal Oxide/Conducting Polymer Hybrids for Application in Supercapacitors, Metal Oxides in Supercapacitors, 2017, 219-245.
[44] Fu L., Qu Q., Holze R., Kondratiev V.V., Wu Y., Composites of metal oxides and intrinsically conducting polymers as supercapacitor electrodes: The best of both worlds?, J. Mater. Chem. A, 2019,7, 14937-14970.